Journal of Hazardous Materials 183 (2010) 189–202

Contents lists available at ScienceDirect

Journal of Hazardous Materials

journal homepage: www.elsevier.com/locate/jhazmat

The comparison of photooxidation processes for the minimization of organic load of colored wastewater applying the response surface methodology

Hrvoje Kusic[a,*], Martina Jovic[a], Natasa Kos[a], Natalija Koprivanac[a], Vedrana Marin[b]

[a] Faculty of Chemical Engineering and Technology, University of Zagreb, Marulicev trg 19, Zagreb 10000, Croatia
[b] Department of Biomedical Sciences, College of Medicine, Florida State University, 1115 West Call Street, Tallahassee, FL, USA

ARTICLE INFO

Article history:
Received 30 March 2010
Received in revised form 30 June 2010
Accepted 2 July 2010
Available online 31 July 2010

Keywords:
Wastewater treatment
Chemical processes
UV irradiation
Azo dye
Optimization
Response surface modeling

ABSTRACT

In this comparative study, the effectiveness of three photooxidation processes (UV/H_2O_2, $UV/S_2O_8^{2-}$ and UV/O_3) for degradation of an azo dye model pollutant was investigated using several process parameters. The process parameters such as initial pH, the concentrations of oxidant in the reactor inlet stream and the type of oxidant were considered. In order to investigate the influence of cross-factor effects of process parameters, the full factorial design was applied with three factors (two numeric and one categorical) at three levels combined with response surface modeling. The ANOVA results (R^2, F, p) showed high accuracy of developed quadratic model for the zero-order mineralization rate constants of AO7 model wastewater. Among process parameters studied, the type of oxidant and the concentration of oxidant were shown to be the most influential parameters of studied photooxidation processes. The highest rate of mineralization of AO7 model wastewater, $k_{obs} = 7.507 \times 10^{-7}$ M s^{-1}, was obtained for UV/O_3 process at the initial pH 10 and oxidant reactor input rate of 0.6 mM min^{-1}. However, when comparing the operating costs for each process studied, it was evident that UV/H_2O_2 process is 1.6 times less expensive than UV/O_3 process considering the mineralization of organic content of AO7 model wastewater.

1. Introduction

Synthetic dyes are present in most spheres of our daily life and their application is continuously growing. They represent a sizable fraction in a vast array of contaminants of anthropogenic origin which inevitably reach our water supplies. The largest group of dyes, presenting more than half of global dye production, are azo dyes with –N=N– unit as the chromophore in the molecular structure [1,2]. Colored wastestreams from azo dye production processes and utilization industries present a major threat to the surrounding ecosystems due to the documented health hazards caused by toxicity and a potentially carcinogenic nature of such organic pollutants [2]. These reasons clearly indicate the necessity for effective dye wastewater treatment prior to release into natural effluents.

Many technologies are available for colored wastewater treatment: adsorption using various adsorbents such as activated carbon, zeolites, polymeric resins, etc.; foam flotation using anionic or cationic surfactants; biodegradation using anareboic/aerobic processes; chemical coagulation/flocculation using various coagulants/flocculants ($AlCl_3$, $FeCl_3$, Levafloc); chemical oxidation by ozone, etc. [3–7]. The major difficulty in the treatment of colored wastewater is related to the ineffectiveness of biological processes, which are usually the most economically suitable processes when compared with other treatment options [8]. Azo dyes are known to be largely non-biodegradable in aerobic conditions and can be reduced to more hazardous intermediates in anaerobic conditions [3,9]. Furthermore, many of above methods merely transfer dyes from one phase to another requiring further treatment [3,8].

The great potential of advanced oxidation processes (AOPs) as destructive, low- or non-waste generating technologies for colored wastewater treatment is well recognized and extensively studied [3,10–12]. AOPs involve the generation of hydroxyl radicals in sufficient quantities to oxidize the majority of organics present in the water matrix [13,14]. Among various types and combinations of AOPs, the chemical and photochemical processes based on the usage of either Fenton type reagent or UV irradiation alongside strong oxidants were shown to be suitable for the degradation of various types of azo dyes [4,11,12,15]. Although efficient and cost effective, the problem often related with the application of Fenton type processes is the relatively high concentration of iron ions in the bulk after the treatment. This disadvantage, which may demand a secondary treatment, can be overcome by the application of photooxidation processes [16]. Like all other AOPs, they are multifactor systems whose efficiency depends on various process parameters, and should be optimized for each particular system [13,14,16]. When AOPS are applied to the treatment of water loaded with complexed pollutants such as dyes, where the identifica-

* Corresponding author. Tel.: +1 385 1 4597 160; fax: +1 385 1 4597 143.
E-mail address: hkusic@fkit.hr (H. Kusic).

0304-3894/$ – see front matter © 2010 Elsevier B.V. All rights reserved.
doi:10.1016/j.jhazmat.2010.07.011

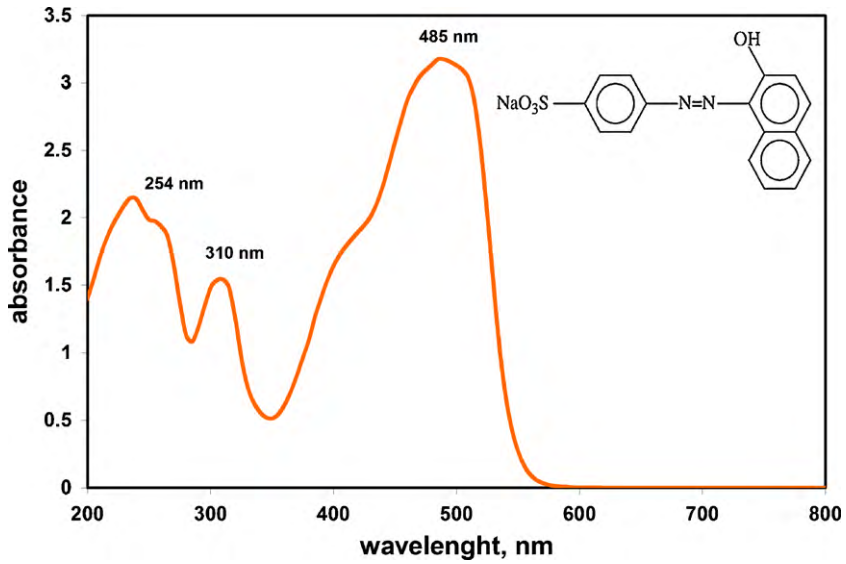

Fig. 1. UV/vis spectra and dye structure of C.I. Acid Orange 7 model pollutant.

tion of degradation intermediates usually requires complicated and costly analytical methods, the traditional experiments could become time and money consuming. Moreover, in order to fully evaluate the effectiveness of such systems, aside from single-factor effects, the cross-factor effects should be taken into consideration as well. Various designs of experiments (DOE) are available for the assessment of system performance depending on process parameters. The application of DOE requires significantly fewer experiments than traditional one-factor-at-a-time-optimization approach which could even result in a misinterpretation of results due to the missing interactions in the overall system [17,18]. One of the methods which takes into account a simultaneous variation of influencing process parameters involving the interactions between them is referred to as a response surface methodology [19]. Hence, various studies showed the advantages of the application of DOE and RSM in the investigation of vast array of issues associated with water pollution and treatment [20–24].

The main goal of this comparative study was to investigate the effectiveness of three photooxidation processes: UV/H_2O_2, UV/$S_2O_8^{2-}$ and UV/O_3 for degradation of an azo dye model pollutant. Their effectiveness strongly depends on pH range of application, the concentrations of oxidant in the reactor inlet stream, and the type of oxidant, and these processes parameters were taken into consideration in the study. In order to consider the combined effects of studied processes parameters, the three-factor (two numeric and one categorical) three-level full factorial experimental design combined with response surface modeling (RSM) and quadratic programming was applied. The same methodology was used to determine the optimal conditions for each of the studied photooxidation processes, which were required for the evaluation on the basis of the cost-effectiveness criteria. The present study was, therefore, undertaken to gain a better understanding in the performance of photooxidation processes as a treatment method for the dye degradation in water matrix, providing as well the comparison of studied processes from both eco- and cost-effectiveness point of view.

2. Materials and methods

2.1. Preparation of dye wastewater and characteristics

Azo dye C.I. Acid Orange 7 (AO7), synthesized previously in our laboratory was used as a model pollutant, according to the procedure described in the literature [25]. The chemical structure of AO7 azo dye, containing a benzene ring substituted by sulfono group (responsible for high solubility in water) and naphthalene structure substituted by hydroxy group which are connected by an azo (–N=N–) bond, is shown in Fig. 1. Model dye wastewater was prepared by dissolving 75 mg L^{-1} of AO7 dye in deionized water with the conductivity of less than 1 μS cm^{-1} (resulting with initial TOC value of 41.87 mg C L^{-1}). All other chemicals used either as oxidants (hydrogen peroxide (H_2O_2), $w = 30\%$, and $Na_2S_2O_8$, p.a.) and auxiliary chemicals for pH adjustment (sodium hydroxide, NaOH, p.a., and sulfuric acid, H_2SO_4, >96%) were purchased from Kemika, Croatia.

2.2. Batch reactor set-up and operation

All experiments were performed in the glass water-jacketed batch reactor with the overall volume of 0.8 L (Fig. 2). The middle of the reactor was occupied with the quartz tube in which a low pressure mercury lamp was placed vertically (typical intensity on 2 cm ≈ 4.4 mW cm^{-2}, UV-C irradiation at 254 nm, UVP-Ultra Violet Products, Cambridge, UK). The value of incident photon flux at 254 nm, 2.34×10^{-6} Einstein s^{-1}, was calculated on the basis of hydrogen peroxide actinometry experiments [26]. The effective irradiation path (L) was 3 cm. The oxidant (H_2O_2, $Na_2S_2O_8$ or O_3) was continuously introduced in the bottom half of the reactor during 60 min of experiments. In cases when H_2O_2 or $Na_2S_2O_8$ were used as oxidants, the stock solutions were prepared in order to match chosen concentrations for full factorial design (Table 1), and were introduced in the reactor using the peristaltic pump (Masterflex, 7518-00, Cole-Parmer, USA). When ozone was used as an oxidant, ozone was generated from pure oxygen, >99.9%, introducing it into the ozone generator, OL80W/FM, OzoneLab, Canada. The outlet gas from the ozononizer was fed into the reactor through a sintered glass plate diffuser located in the bottom half of the reactor. The rate of ozone generation was varied in order to match chosen concentrations for full factorial design (Table 1). Initial pH values and reactor input oxidant rate ranged from 3 to 10 and 0.1 mM min^{-1} to 0.6 mM min^{-1}, respectively, in order to achieve requirements for the desired full factorial design (Table 1). Initial pH was adjusted with the addition of 0.1 M NaOH or 0.1 M H_2SO_4. Added quantities of H_2SO_4, NaOH and stock solutions of oxidants (H_2O_2 or $Na_2S_2O_8$), were negligible in comparison to the total volume of treated reaction mixture. The total volume of the treated

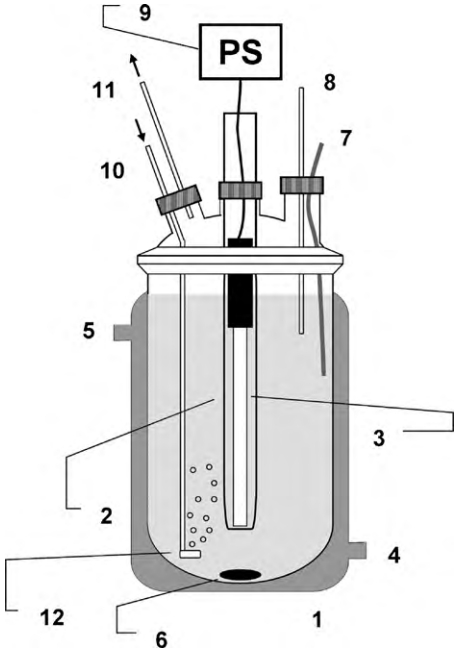

Fig. 2. Schematic diagram of experimental set-up for applied photooxidation processes. (1) Glass water-jacketed reactor, (2) quartz jacket, (3) UV lamp, (4) and (5) cooling water inlet and outlet, (6) magnetic stirring bar, (7) sampling port, (8) thermometer, (9) power supply, (10) gas diffusing plate, (11) and (12) ozone inlet and outlet.

solution was 0.5 L in all cases, while the mixing of the solution was provided by magnetic stirring. Experiments were carried out at 24.2 (±0.2) °C. The duration of each experiment was 60 min; samples were taken periodically from the reactor (0, 10, 20, 30, 40, 50 and 60 min) and immediately analyzed thereafter. All experiments were performed in triplicates and averages are reported, whilst the reproducibility of experiments was >95%.

2.3. Analytical methods

The degradation of AO7 dye was monitored by UV/vis spectrophotometer, Perkin Elmer Lambda EZ 201, scanning UV and visible spectra in the range from 200 to 800 nm. The degradation degree of AO7 was determined on the basis of the decrease of peaks on several characteristics wavelengths: (i) at λ_{max} = 485 nm, pick corresponding to dye chromophore (decolorization); (ii) at λ_{max} = 310 nm, pick corresponding to naphthalene structure and (iii) at λ_{max} = 254 nm, characteristic for aromatic structures in dye molecule (aromaticity removal) (UV/vis spectra of AO7 dye is presented in Fig. 1). The mineralization degree of AO7 was determined by measuring the total organic content (TOC) of model wastewater during the experiments, which was performed by Total Organic Carbon analyzer, TOC-V_{CPN}, Shimadzu, Japan. Handylab pH/LF portable pH-meter, Schott Instruments GmbH, Mainz, Germany, was used for pH measurements.

2.4. Response surface methodology

In order to compare the process effectiveness depending on chosen process parameters (pH range of application and the concentration of oxidant in the reactor inlet stream) and the type of oxidant the three-factor (two numeric and one categorical) three-level full factorial experimental design combined with response surface modeling (RSM) and quadratic programming was used. The same methodology was used to determine the optimal conditions of each of studied photooxidation process (UV/H_2O_2, UV/$S_2O_8^{2-}$ and UV/O_3) for the maximal degradation of AO7. RSM consists of a group of empirical techniques directed to evaluate the relationships between a cluster of controlled experimental factors determined by an appropriate experimental design and measured responses according to one or more selected criteria [17–19]. The first step of RSM includes an introduction of a suitable approximation in order to find the true relationship between the dependent variable (chosen response) and the set of independent variables (factors). If the shape of true response surface is insufficient, the preliminary model (usually a first-order model) is upgraded by adding high-order terms into it [19,21]. In the next step, the behavior of the system is explained by the following quadratic Eq. [19]:

$$Y = \beta_0 + \sum_{i=1}^{k}\beta_i X_i + \sum_{i=1}^{k}\beta_{ii} X_i^2 + \sum_{i=1}^{k}\sum_{j=1}^{k}\beta_{ij} X_i X_j + \varepsilon' \quad (1)$$

Y is the chosen process response, i.e. dependent variable; k represents the number of patterns; i and j are index numbers for patterns; β_0 is the offset term, X_i, ..., X_k are coded independent variables; β_i is the first-order, i.e. linear, effect; β_{ii} is the second-order, i.e. quadratic, effect; while β_{ij} represents the interaction effect and ε' is the random error allowing the discrepancies or uncertainties between predicted and observed values. When developing the model presented by Eq. (1), the natural, i.e. uncoded, independent variables should be transformed in dimensionless coded values at levels according to the chosen experimental design (e.g. in our case three levels −1, 0 and 1). The chosen effects in the study influencing the degradation of AO7 in model wastewater by applied photooxidation processes are the initial pH value (X_1), the concentration of the oxidant reactor inlet stream (X_2) and the type of oxidant (X_3). The influence of chosen process parameters was tested with the zero-order mineralization rate constant of AO7 dye wastewater (Y). The experimental range and levels of independent variables involved in the study, including observed and predicted values of studied response by developed quadratic models are presented in Table 1. The optimal conditions for each of studied photooxidation processes in the experimental range of investigated processes parameters were determined using RSM calculating separately the quadratic models for each process using two-factor three-level full factorial design. The values of predicted responses are listed in Table 1 as well.

2.5. Statistical analysis

The fitting of models was calculated using the coefficient of determination R-squared (R^2) and the analysis of variance (ANOVA). For the purpose of ANOVA, regression and graphical analyses of obtained data the software packages STATISTICA 8.0, StatSoft Inc., USA, and Design-Expert 8.0, StatEase, USA, were used. The optimal values of studied process parameters predicted by RSM were calculated using numerical technique built-in software *Mathematica 6.0* (Wolfram Research, Champaign, IL).

3. Results and discussion

3.1. Development of RSM-based model

The full factorial design including three factors (two numeric and one categorical) at three levels was performed in order to compare effectiveness of studied photooxidation processes (UV/H_2O_2, UV/$S_2O_8^{2-}$ and UV/O_3) for the degradation of AO7 model wastewater. Three process parameters taken into consideration were: initial pH of application, the concentration of oxidant in the reactor inlet stream, and the type of oxidant. It should be noted that the concentration of oxidant on the top level in the reactor inlet stream

Table 1
Full factorial design matrix with three independent variables (including one categorical) expressed in coded and natural units, experimentally obtained values of dye degradation and values of observed and predicted responses.

Run	Variables					Experimental					Response, Y		
	Variable 1, X_1		Variable 2, X_2		Variable 3, X_3	Overall dye degradation, norm					$k_{obs} \times 10^{-7}$ ($M\,s^{-1}$)		
	Coded	Uncoded: pH_0	Coded	Uncoded: oxidant input rate ($mM\,min^{-1}$)	Categorical: oxidant type	A_{485}	A_{310}	A_{254}	ΔTOC (mineralization)		Power transform: $\sqrt{Y}$		
									Final	$k_{obs} \times 10^{-7}$ ($M\,s^{-1}$)	Obs.	Pred.[a]	Pred.[b]
1	0	6.5	0	0.35	H_2O_2	0.78	0.33	0.06	0.153	1.387	1.18	1.11	1.18
2	−1	3	−1	0.1	$Na_2S_2O_8$	0.68	0.46	0.05	0.176	1.582	1.26	1.17	1.20
3	−1	3	1	0.6	H_2O_2	0.87	0.43	0.01	0.150	1.456	1.21	1.21	1.23
4	−1	3	0	0.35	$Na_2S_2O_8$	0.98	0.63	0.09	0.223	2.206	1.49	1.49	1.53
5	0	6.5	0	0.35	O_3	1.0	0.97	0.91	0.332	3.037	1.74	1.83	1.74
6	0	6.5	−1	0.1	O_3	0.98	0.77	0.52	0.140	1.324	1.15	1.18	1.13
7	1	10	−1	0.1	O_3	1.0	0.98	0.94	0.185	1.811	1.35	1.35	1.39
8	0	6.5	0	0.35	$Na_2S_2O_8$	0.74	0.46	0.06	0.205	2.086	1.44	1.32	1.36
9	0	6.5	−1	0.1	H_2O_2	0.47	0.20	0.05	0.125	1.226	1.11	1.07	1.14
10	1	10	1	0.6	H_2O_2	0.86	0.41	0.05	0.086	0.837	0.91	1.02	0.93
11	1	10	0	0.35	H_2O_2	0.81	0.37	0.05	0.083	0.831	0.91	0.95	0.91
12	1	10	1	0.6	$Na_2S_2O_8$	0.99	0.63	0	0.217	2.160	1.47	1.48	1.48
13	−1	3	0	0.35	O_3	1.0	0.99	0.94	0.224	2.189	1.48	1.58	1.54
14	−1	3	0	0.35	H_2O_2	0.70	0.36	0.03	0.157	1.415	1.19	1.23	1.19
15	−1	3	1	0.6	O_3	1.0	1.0	0.98	0.574	4.997	2.24	2.17	2.21
16	0	6.5	1	0.6	O_3	1.0	1.0	0.98	0.641	5.960	2.44	2.46	2.45
17	0	6.5	−1	0.1	$Na_2S_2O_8$	0.40	0.29	0	0.068	0.636	0.80	0.96	0.95
18	−1	3	1	0.6	$Na_2S_2O_8$	0.95	0.61	0.09	0.311	3.060	1.75	1.79	1.75
19	1	10	−1	0.1	H_2O_2	0.38	0.23	0.03	0.082	0.825	0.91	0.87	0.89
20	1	10	0	0.35	O_3	1.0	0.98	0.94	0.479	4.332	2.08	2.04	2.04
21	1	10	1	0.6	O_3	1.0	1.0	0.99	0.783	7.507	2.74	2.71	2.75
22	−1	3	−1	0.1	O_3	1.0	0.86	0.65	0.129	1.169	1.08	0.97	1.05
23	1	10	0	0.35	$Na_2S_2O_8$	0.63	0.41	0.06	0.129	1.307	1.14	1.10	1.18
24	0	6.5	1	0.6	$Na_2S_2O_8$	0.99	0.64	0.03	0.272	2.648	1.63	1.66	1.62
25	1	10	−1	0.1	$Na_2S_2O_8$	0.13	0.14	0	0.053	0.481	0.69	0.70	0.61
26	−1	3	−1	0.1	H_2O_2	0.50	0.24	0.04	0.141	1.347	1.16	1.23	1.14
27	0	6.5	1	0.6	H_2O_2	0.86	0.40	0.10	0.178	1.559	1.25	1.14	1.21

[a] Predicted by model M1.
[b] Predicted by models M2, M3, and M4–depending on the type of oxidant.

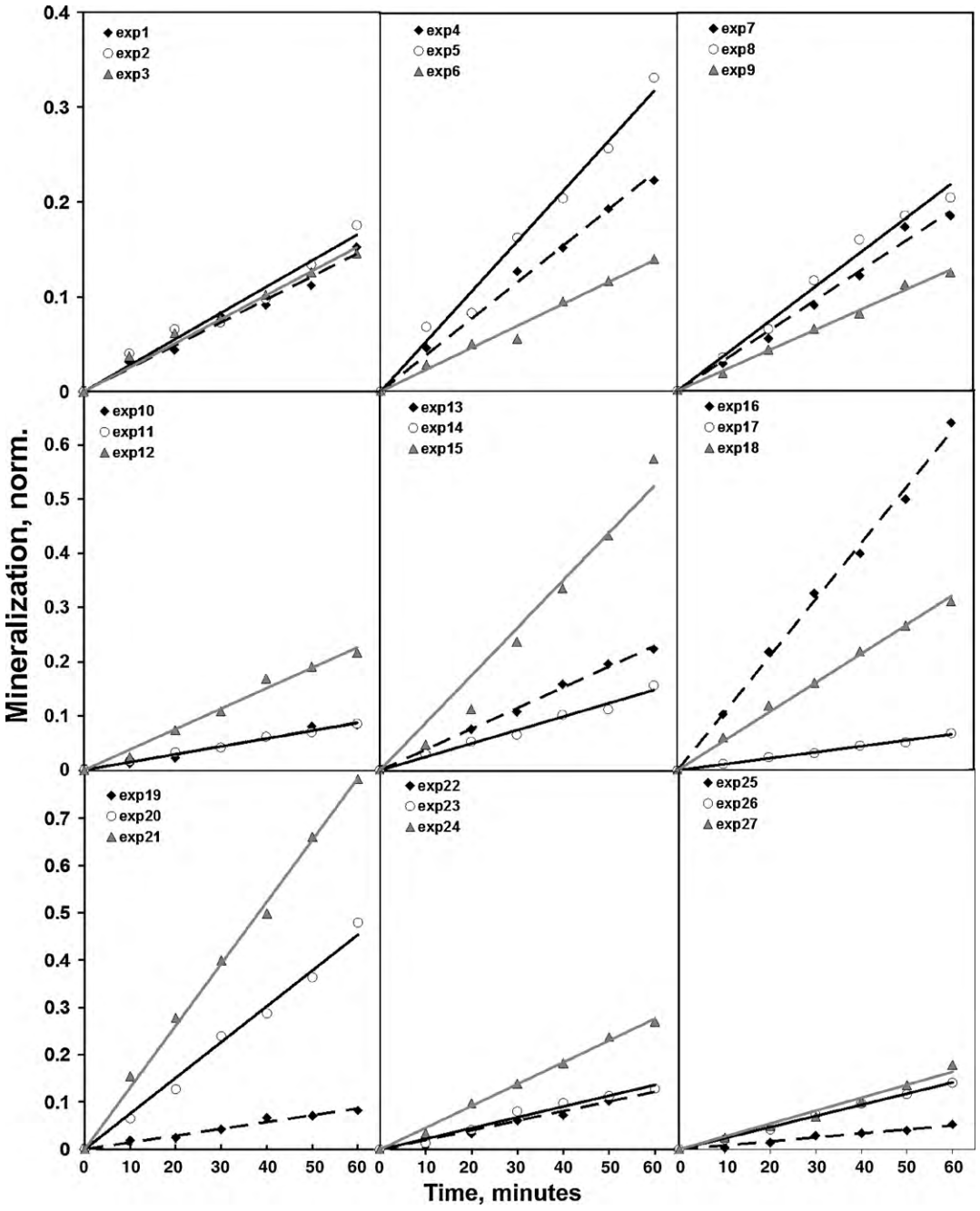

Fig. 3. Graphical estimation of zero-order kinetic for the experimentally obtained values of TOC removal by studied photooxidation processes at set conditions given in Table 1.

was limited by the maximal possible value which can be produced by used ozone generator. The process effectiveness was evaluated through following: the decolorization of AO7 model wastewater, the degradation of dye monitored through the decrease of absorbance of characteristic peaks of AO7 dye molecule and mineralization of organic content of AO7 model dye wastewater. In order to indirectly introduce the fourth parameter in the applied experimental design, i.e. the treatment time, the performance of RSM model on the rate constants for the above mentioned dye degradation indicators was tested. According to Connors [27], the possibility for comparing the reactions and their rates is based on the fact that, the reaction order has to be determined and then if all of them can be fitted to the same order, the rate constants can be easily calculated by the linear regression and compared. Therefore, the obtained values of the chosen indicators through the observed treatment time were fitted using integrated equations for the several integral orders of reactions (zero, first and second) displayed by different functional dependences of concentration on time [27]. It was determined that the most of the chosen indicators of process effectiveness can be fitted to the first- or even the zero-order kinetics. The decolorization of AO7 model wastewater was not taken into consideration as a possible response (i.e. dependent variable in RSM) due to the large differences between the obtained results, e.g. in processes using ozone as an oxidant, decolorization was rather fast demanding almost on-line measuring, while in a case where $Na_2S_2O_8$ was used as oxidant (run #25, Table 1) only 15% of decolorization was achieved after 60 min of treatment. Furthermore, it was shown that dye

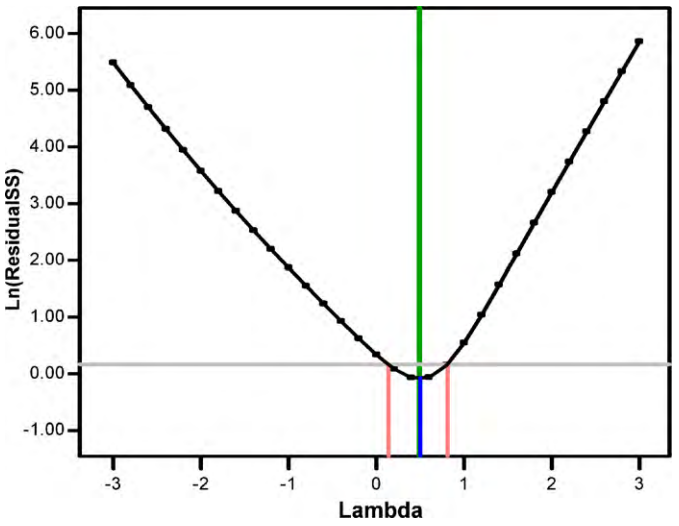

Fig. 4. Box–Cox plot of model transformation for zero-order mineralization rates of AO7 model wastewater by studied photooxidation processes.

chromophore is less sensitive to the attack of oxidative/reductive species and cannot be clear representative of system behavior when other indicators of dye degradation are available (e.g. TOC, COD) [4,10,12]. Among other indicators of process effectiveness monitored, the mineralization rates of AO7 model wastewater were shown to be the most appropriate responses for describing the system behavior in response to chosen process parameters. Results of the performed linear regression on the obtained values of mineralization extents of AO7 model wastewater at the set experimental conditions by applied full factorial design (Table 1) are shown in Fig. 3. It can be seen that experimental data fitted are in good agreement with the zero-order kinetic (the coefficients of linear regression (R^2_{rates}) ranged from 0.967 to 0.998). Obtained rate constants of AO7 mineralization (k_{obs}) ranged from 0.481 to 7.507×10^{-7} M s^{-1}. Thus, the mineralization rate constants were chosen as appropriate responses for evaluating the effect of studied parameters by RSM (Table 1). It should be noted that responses (zero-order mineralization rate constants of AO7) were checked for the maximum and minimum ratios. Generally, a ratio greater than 10 indicates a higher likelihood that the transformation of the response may improve the model [28]. In our case, the ratio of maximum to minimum response was 15.6 indicating that the transformation is required. In order to obtain the appropriate response a Box-Cox plot was used (Fig. 4). Generally, the natural logarithmic value of the residual sum of squares *vs.* λ (lambda) should dip fairly steeply with a minimum in the region of the optimum value [29]. In the case of square root transform, lambda is 0.5. The used quadratic model showed that the minimum and maximum confidence intervals are 0.14 and 0.81, respectively (Fig. 4). The current point of confidence interval (0.5) lies very closely to the model design value of 0.49 (Fig. 4), indicating the appropriate squared root transformation of response Y used. Therefore, in the further application of RSM a square root response ($Y' = \sqrt{Y}$) of originally calculated mineralization rate constants were used (Table 1).

In Table 1 are listed statistical combinations, i.e. design matrix, for full factorial design applied. As it was stated above, RSM is based on the estimation of parameters which indicate an empirical relationship between the response and the input variables. When multiple regression analysis (MRA) is applied on the design matrix and obtained values for chosen response, a fitted second–order polynomial equation (model M1) was established to predict the zero-order mineralization rate constants of AO7 by studied photooxidation process:

$$Y' = \sqrt{Y} = 1.42 - 0.035 \times X_1 - 0.023 \times X_1^2 + 0.34 \times X_2 - 0.0097 \times X_2^2 + 0.41 \times X_3[1] - 0.31 \times X_3[2] + 0.04 \times X_1 \times X_2 + 0.26 \times X_1 \times X_3[1] - 0.10 \times X_1 \times X_3[2] + 0.30 \times X_2 \times X_3[1] - 0.31 \times X_2 \times X_3[2] \quad (2)$$

Table 2
Analysis of variance (ANOVA) of the response surface model M2 for the prediction of zero-order mineralization rate constant of AO7 model wastewater by applied photooxidation processes.

Factors (coded)	Statistics				
	SS	df	MSS	*F*	*p*
Model	6.35	11	0.58	66.58	<0.0001*
X_1	0.023	1	0.023	2.60	0.1279
X_1^2	3.28×10^{-3}	1	3.28×10^{-3}	0.38	0.5480
X_2	2.09	1	2.09	240.71	<0.0001*
X_2^2	5.7×10^{-4}	1	5.7×10^{-4}	0.066	0.8012
X_3	2.47	2	1.24	142.5	<0.0001*
$X_1 \times X_2$	0.02	1	0.02	2.26	0.1538
$X_1 \times X_3$	0.64	2	0.32	36.76	<0.0001*
$X_2 \times X_3$	1.11	2	0.55	63.9	<0.0001*
Residual	0.13	15	8.67×10^{-3}		
Total	6.48	26			

* $p < 0.05$ are considered as significant.

However, coefficients for multi-level categorical factors (as used in our case to describe the influence of oxidant type) are not easy and simple to interpret. They do not have the physical meaning, but do have mathematical meaning. For instance, $X_3[1]$ is a difference of level 2 from the overall average, while $X_3[2]$ is a difference of level 3 from the overall average. In general case, $X_i[n]$ is a difference of level $(n+1)$ from the overall average. Thereby, the interpretation of the model results over model graphs is recommended [28]. The analysis of variance (ANOVA), considered as the most important test for the evaluation of significance of developed model [19,21,22], was applied to test the significance of the fit of the model M1 (Eq. (2)). The results are presented in Table 2 (numerically) and Fig. 5 (graphically). According to the calculated Fisher *F*-test value alongside a very low probability value ($p_{model} < 0.0001$), it can be concluded that M1 is highly significant (Table 1). The fitting of model to the empirical data was tested by calculating the regression coefficient (R^2). Rather high regression coefficient ($R^2 = 0.9799$) alongside the high value of adjusted regression coefficient ($R^2_{adj} = 0.9652$), which is moreover very close to R^2, indicates the capability of developed model M1 to satisfactorily describe the system behavior within the investigated range of operating parameters. According to the literature [21,22], R^2_{adj} corrects R^2 for the sample size and the number of terms in the model; e.g. many terms in the model and small sample size might cause that $R^2_{adj} \ll R^2$, which was not obtained in our study. The high correlation between observed and predicted data can be seen from the graphical interpretation given in Fig. 5(A). It is evident that the points or point clusters are placed very closely to the diagonal line as a result of their low discrepancies. The important information on the model performance is summarized in residuals (i.e. difference between observed and predicted values) providing a clear view for any discrepancy in fit to the model. Hence, two plots related to residuals: the normal probability plot of residuals and the plot of internally studentized residuals *vs.* predicted values are presented in Fig. 5(B) and (C), respectively. In normal probability plot, similar to the observed *vs.* predicted values plot ((Fig. 5(A)), points or point clusters are placed closely to the diagonal line (Fig. 5(B)). This observation leads to the conclusions that there are no serious violations in the assumptions that errors are

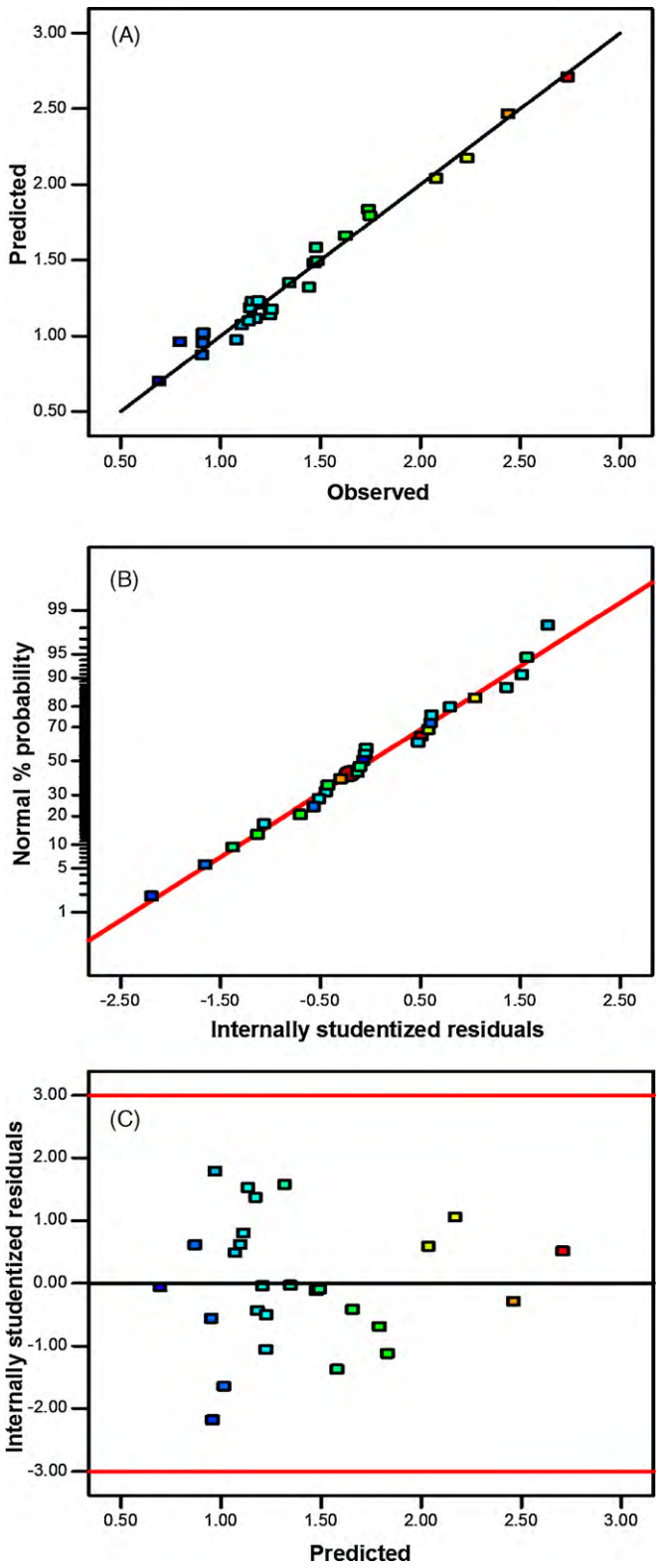

Fig. 5. Residual diagnostics of model M1 for the prediction of zero-order mineralization rate constant of AO7 model wastewater by studied photooxidation processes: (A) observed *vs.* predicted plot, (B) normal probability plot, and (C) internally studentized residuals *vs.* predicted values plot.

normally distributed and independent of each other that the error variances are homogeneous and that residuals are independent. The plot presented in Fig. 5(C) tests the assumption of constant variance. The points are randomly scattered and all values lie within the range of −2.19 and 1.78 (values between −3 and +3 are considered as the top and bottom outlier detection limits). According to the layouts of the plots presented in Fig. 5, it was concluded that used response transformation was appropriate, that there was no apparent problem with normality, and that developed quadratic model M1 is successful in capturing the correlation between the influencing parameters of studied photooxidation processes.

3.2. Effects of model components and their interactions

Since it was determined that the model M1 is significant (*F* and *p* values, Table 2) and that its predictivity of investigated systems behavior is rather accurate (R^2 and R^2_{adj}, graphical results in Fig. 5), the next step of the study was to determine which model terms are significant for its performance. Here, it was expected to gain insight into which of the investigated process parameters are highly influential on the mineralization rates of AO7 model wastewater by studied photooxidation processes. This is evaluated on the basis of *F* and *p* values listed in Table 2 for each of M1 model terms (linear, quadratic and interaction). It is evident that significant terms are those, which have a *p* value <0.05 [28]: X_2 and X_3, representing the linear terms for the concentration of oxidant reactor inlet stream and the type of oxidant, respectively. Both of these terms are characterized by a very low *p* value (<0.0001). The same low probability values are obtained for other two model terms: $X_1 \times X_3$ and $X_2 \times X_3$, standing for the interaction terms between initial pH value and the type of oxidant, and the concentration of oxidant reactor inlet stream and the type of oxidant, respectively. These results can easily be associated with the physical meaning of mentioned parameters. The concentration of oxidant reactor inlet stream is important process parameter since its higher rate in reactor inlet stream would supply the system with more oxidant providing more source for the generation of reactive species (e.g. hydroxyl radicals ($HO^\bullet$), sulfate radicals ($SO_4^{\bullet-}$)), according to the following equations ((3)–(5)) [16,30]:

$$H_2O_2 \xrightarrow{h\nu} 2HO^\bullet \quad (3)$$

$$S_2O_8^{2-} \xrightarrow{h\nu} 2SO_4^{-\bullet} \quad (4)$$

$$O_3 + H_2O \xrightarrow{h\nu} 2HO^\bullet + O_2 \quad (5)$$

Furthermore, in the case of ozone, its higher rate in reactor inlet stream would provide more ozone in reactor which can degrade AO7 model organic pollutant directly (Eq. (6)) or indirectly by forming the radical species (Eq. (7)) [16,31,32]:

$$O_3 + AO7 \rightarrow \text{products} \quad (6)$$

$$O_3 + H_2O \xrightarrow{OH^-} HO^\bullet + AO7 \rightarrow \text{products} \quad (7)$$

It should be noted that control experiments showed that the direct oxidation of AO7 by other two oxidants (H_2O_2 and $Na_2S_2O_8$) is not possible, providing only negligible changes in UV/vis spectra of studied organic pollutant in the absence of UV irradiation (results not shown). The importance of the type of oxidant as a process parameter can be clearly drawn from the capability of studied oxidants to directly oxidize the AO7. The redox potential of studied oxidants followed decreasing order: ozone (2.07 V) > peroxidisulfate (2.01) > hydrogen peroxide (1.77 V) [16,33]. However, all of these redox potentials are significantly lower than those of $HO^\bullet$ (2.8 V) and $SO_4^{\bullet-}$ (2.4 V) [16,34], indicating that degradation by radical species generated either by direct photolysis of oxidants (Eqs. (3)–(5)) or in the case of ozone catalyzed by

Table 3
Analysis of variance (ANOVA) of the response surface models M2, M3 and M4 for the prediction of zero-order mineralization rate constants of AO7 model wastewater by UV/H_2O_2, $UV/S_2O_8^{2-}$ and UV/O_3 processes, respectively.

Model	Process	Source	Statistics						
			SS	df	MSS	F	p	R^2	R^2_{adj}
M2	UV/H_2O_2	Model	0.68	5	0.14	16.44	0.022*	0.965	0.906
		Residuals	0.025	3	8.28×10^{-3}				
		Total	0.71	8					
M3	$UV/S_2O_8^{2-}$	Model	5.89	5	1.18	19.55	0.017*	0.970	0.921
		Residuals	0.18	3	0.06				
		Total	6.07	8					
M4	UV/O_3	Model	39.81	5	7.96	212.12	0.0005*	0.997	0.993
		Residuals	0.11	3	0.038				
		Total	39.92	8					

* $p < 0.05$ are considered as significant.

OH^- (Eq. (7)) strongly dominated over that via direct oxidation. This fact brings forth the capability of studied oxidants to generate the reactive radical species under UV light (Eqs. (3)–(5)). According to the literature [16], the decomposition of any chemical specie under UV irradiation highly depend on the several factors: the concentration (c) of parent specie (i) and its decomposition by-products (j), physical parameters of species in the system such as their quantum yields (Φ) and extinction coefficients (ε), reactor geometry i.e. effective path of radiation (L) and intensity of incident radiation (I_0) (Eq. (8)):

$$-\frac{dc_i}{dt} = \phi_i F_i I_o \left(1 - \exp(-2.303 \cdot L \cdot \sum \varepsilon_j c_j)\right) \quad (8)$$

where $F_i = \varepsilon_i c_i / \sum \varepsilon_i c_j$.

Since the several of mentioned factors where the same for all three studied systems (c, L and I_0), it is clear that the differences in physical parameters of studied oxidants (Φ and ε) influenced processes effectiveness. The values of extinction coefficients (ε) at the wavelength of irradiation (254 nm) used in the study followed decreasing order: $3300\ M^{-1}cm^{-1}$ (O_3) > $47.45\ M^{-1}cm^{-1}$ ($S_2O_8^{2-}$) > $18.6\ M^{-1}cm^{-1}$ (H_2O_2). The same decreasing order is valid for values of quantum yields: 0.62 mol Einstein^{-1} (O_3) > 0.55 mol Einstein^{-1} ($S_2O_8^{2-}$) > 0.5 mol Einstein^{-1} (H_2O_2) [16,30,35]. It is evident from the presented Φ and ε values that oxidant type strongly influence the generation of radical species, i.e. the overall process effectiveness. Guittonneau et al. [36,37] reported that the decay rate of ozone under UV light is about a factor of 1000 higher than that of hydrogen peroxide. According to the differences given for ε and Φ between ozone and peroxidisulfate, the similar assumption can be made for that comparison too; ozone decay rate is significantly higher than that of peroxidisulfate. The above stated can be proven by the calculated mineralization rate constants for the corresponding processes, i.e. those at the same set conditions but with different oxidant type. This is particularly clear when comparing the cases at pH values either 3 or 6.5 due to the fact that the influence of indirect ozonation providing additional HO• was minor in those cases (Table 1 and Fig. 3). It can be observed that processes using ozone as an oxidant are significantly efficient than those using other two oxidants. At the highest used oxidant rate (0.6 mM min^{-1}) runs #15 and #16 using ozone at pHs 3 and 6.5, respectively, yielded both with 100% decolorization alongside 57.4 and 64.1% mineralization after 1 h treatment, respectively (Table 1). The corresponding processes using peroxidisulfate as oxidant yielded with 95% 31.1% (run #18, pH 3) and 99% decolorization and 27.2% mineralization (run #24, pH 6.5) (Table 1). The corresponding processes using hydrogen peroxide provided even lower effectiveness of AO7 model wastewater treatment (Table 1, runs #3 and #27). Other two significant model terms in M1, $X_1 \times X_3$ and $X_2 \times X_3$ (Table 2), are closely correlated with the type of oxidant. They represent the interaction terms between initial pH value and the type of oxidant ($X_1 \times X_3$), and the concentration of oxidant reactor inlet stream and the type of oxidant ($X_2 \times X_3$). The influence of interactions between the initial pH and type of oxidant is especially important when ozone is used as an oxidant due to the fact that indirect ozonation (ozone catalyzed by OH^- (7)) provides additional source of HO• in the system and increasing the overall process effectiveness. This can be observed from the comparison of processes performed at basic, neutral or acidic initial pHs: run #21 (pH 10) with $k_{obs} = 7.507 \times 10^{-7}\ M\,s^{-1}$ and runs #15 (pH 3) and #16 (pH 6.5) with $k_{obs} = 4.997 \times 10^{-7}\ M\,s^{-1}$ and $k_{obs} = 5.960 \times 10^{-7}\ M\,s^{-1}$, respectively (Table 1). This model term, $X_1 \times X_3$, showed a high influence on the UV/H_2O_2 process due to the fact that hydrogen peroxide dissociates in alkaline media, resulting with lower process efficiency [12,20]. Therefore, the mineralization rates in corresponding processes using H_2O_2 at pHs 3 and 6.5 were significantly higher than those in alkaline media (e.g. comparison of runs #3 and #27 with the run #10) (Table 1). Similar system behavior is observed in the case of peroxidisulfates (e.g. runs #18, #24 and #12 at pHs 3, 6.5 and 10, respectively). The importance of the other interaction term $X_2 \times X_3$ can be attributed to the above mentioned. This term represents the correlation between the input oxidant rate; higher rate results with more oxidant in the system and more reactive species, and the type of oxidant; large differences in physical parameters such as quantum yields and extinction coefficients between studied oxidants indicated on the high significance of oxidant type.

3.3. Response surface diagrams and contour plots

In order to determine the optimal conditions within the investigated ranges of studied process parameters (pH and oxidant input rate) for each of applied photooxidation processes, the RSM is applied on two-factor three-level full factorial design for each oxidant type. First studied process was UV/H_2O_2. The derived RSM model, M2, for UV/H_2O_2 process is presented by Eq. (9), and predicted values are summarized in Table 1. Additionally, the ANOVA results and regression coefficients are presented in Table 3, while the graphical estimation of the model performance and the contribution of the terms in model M2, i.e. process parameters studied, are shown in Fig. 6.

$$Y = 1.39 - 0.288 \times X_1 - 0.272 \times X_1^2 + 0.075 \times X_2 - 0.0029 \times X_2^2 + 0.024 \times X_1 \times X_2 \quad (9)$$

The predicted values by M2 are very close to those obtained M1 (Table 1). The regression coefficients are rather high and close to each other: $R^2 = 0.965$ and $R^2_{adj} = 0.906$ (Table 3). The model accuracy in describing the behavior of UV/H_2O_2 process can be seen

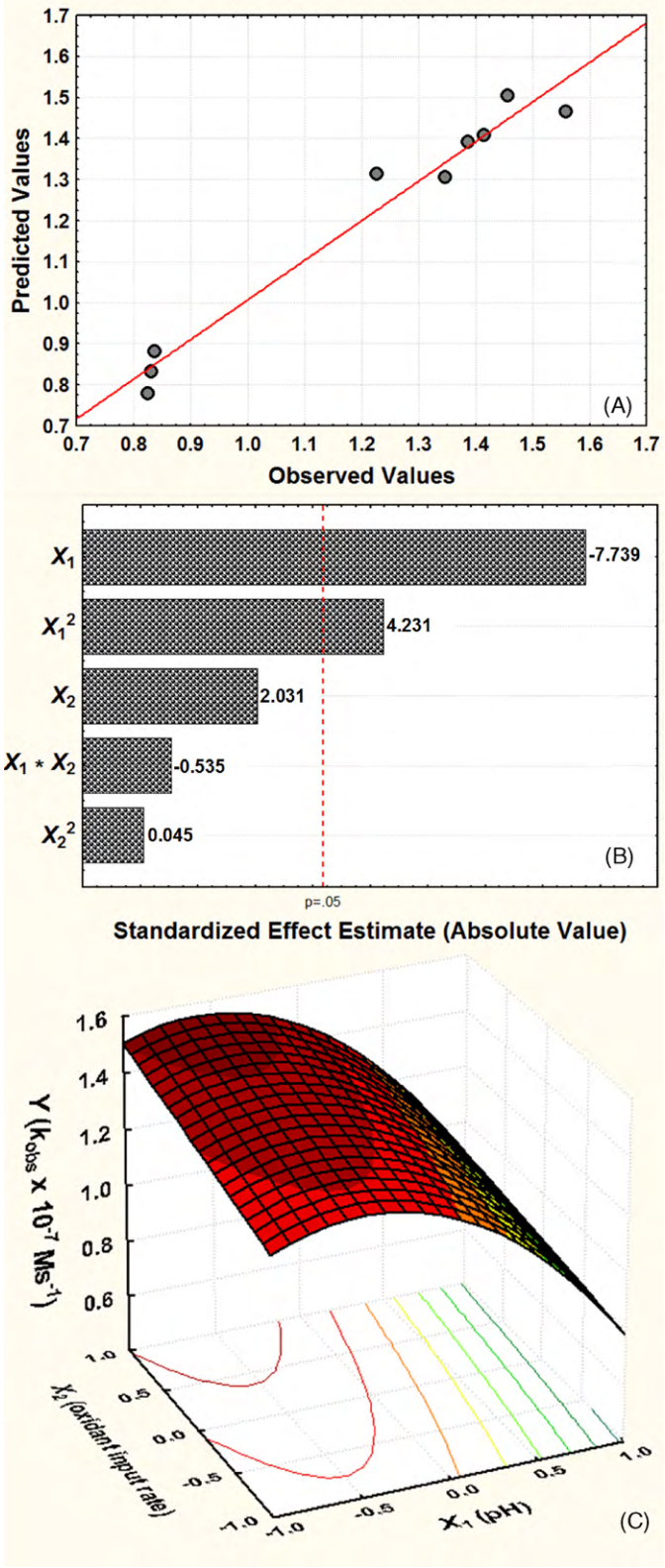

Fig. 6. Graphical evaluation of model M2 performance for the prediction of zero-order mineralization rate constant of AO7 model wastewater by UV/H_2O_2 process: (A) observed *vs.* predicted plot, (B) Pareto chart, and (C) 3D response surface and contour plot.

from the plot of observed *vs.* predicted values (Fig. 6(A)). Points and point clusters are placed closely to the diagonal line indicating the low values of residuals. According to F and p values (16.44 and 0.022, respectively) listed in Table 3, the model M2 can be characterized as significant. The significance of each of the term in model M2 is presented through Pareto Chart (Fig. 6(B)). Generally, the length of each bar in Pareto chart indicates the standardized effect of that term on the response Y [21]. The bars for model terms X_1 and X_1^2 (both corresponding to initial pH) exceeded the reference line ($p = 0.05$) which indicates their significance on the prediction of mineralization rate of AO7 by M2 (Fig. 6(B)). Such observation is slightly in contrast with the results obtained by overall model M1 where neither linear of quadratic model terms corresponding to initial pH value were shown to be significant (Table 2). Accordingly, it was concluded that although M1 accurately predicted AO7 mineralization rate constants by studied photooxidation processes, when observing each process separately, different parameters could be indicated as significant. The plausible explanation for the insignificance of the concentration of oxidant in M2 could be a rather low overall concentration of oxidant (i.e. H_2O_2) introduced in the system after 1 h; only 36 mM in the case of the highest input rate. However, it should be noted that the large portion of it was consumed/decomposed during the treatment. According to our previous studies and literature findings [12,20,38], only the pollutant/H_2O_2 ratios ranging from 1: 100 to 1: 200 yielded with higher mineralization of organic pollutants. In this study the highest possible ratio was 1: 10. The high importance of initial pH value and insignificance of input oxidant rate (within the studied range) on the AO7 mineralization rate can be also observed from the corresponding 3D and contour plots (Fig. 6(C)). AO7 mineralization rate highly depends on initial pH, resulting with rather low mineralization rate of AO7 model wastewater in strong basic conditions, presumably due to the increased dissociation of added H_2O_2 at elevated pHs [12]. According to the contour plot (Fig. 6(C)), the most suitable conditions for AO7 mineralization within investigated range were shown to be at the initial pH range around 4.75 (coded $X_1 = -0.5$) and the highest used oxidant input rate. In order to determine the exact values of optimal conditions within the investigated range, the numerical technique built-in software *Mathematica 6.0* (Wolfram Research, Champaign, IL) was used. The initial pH 4.5 (coded $X_1 = -0.573$) and the concentration of oxidant in the reactor inlet stream of 0.6 mM min^{-1} (coded $X_2 = 1$) were shown as optimal predicting the mineralization of AO7 with the rate constants $k_{obs} = 1.555 \times 10^{-7}$ M s^{-1}.

Graphical estimations for model M3 predicting AO7 mineralization rate constants in dependence on initial pH and oxidant input rate for UV/$S_2O_8^{2-}$ process are presented in Fig. 7. Model M3 (Eq. (10)) was developed analogously to that for UV/H_2O_2 process (M2).

$$Y = 1.86 - 0.483 \times X_1 - 0.0095 \times X_1^2 + 0.862 \times X_2 - 0.105 \times X_2^2 + 0.050 \times X_1 \times X_2 \quad (10)$$

The ANOVA results for M3 and predicted values by it are summarized in Tables 3 and 1, respectively. Model M3 can be marked as significant ($F = 19.55$ and $p = 0.017$), showing even higher regression coefficients ($R^2 = 0.970$ and $R^2_{adj} = 0.921$) than obtained for model M2 (Table 3). The high correlation of observed and predicted values is shown in Fig. 7(A); the points are located closely to the diagonal line. The significance of M3 model components is estimated using Pareto chart (Fig. 7(B)). The bars of linear model terms X_1 and X_2 crossed the reference $p = 0.05$ line, marking them as significant for the predictivity of AO7 mineralization rate constants by M3. These results indicate that even a linear model could provide successful results in predicting UV/$S_2O_8^{2-}$ system behavior. However, the quadratic one was applied in order to compare the results with those obtained by model M1. The significance of only linear

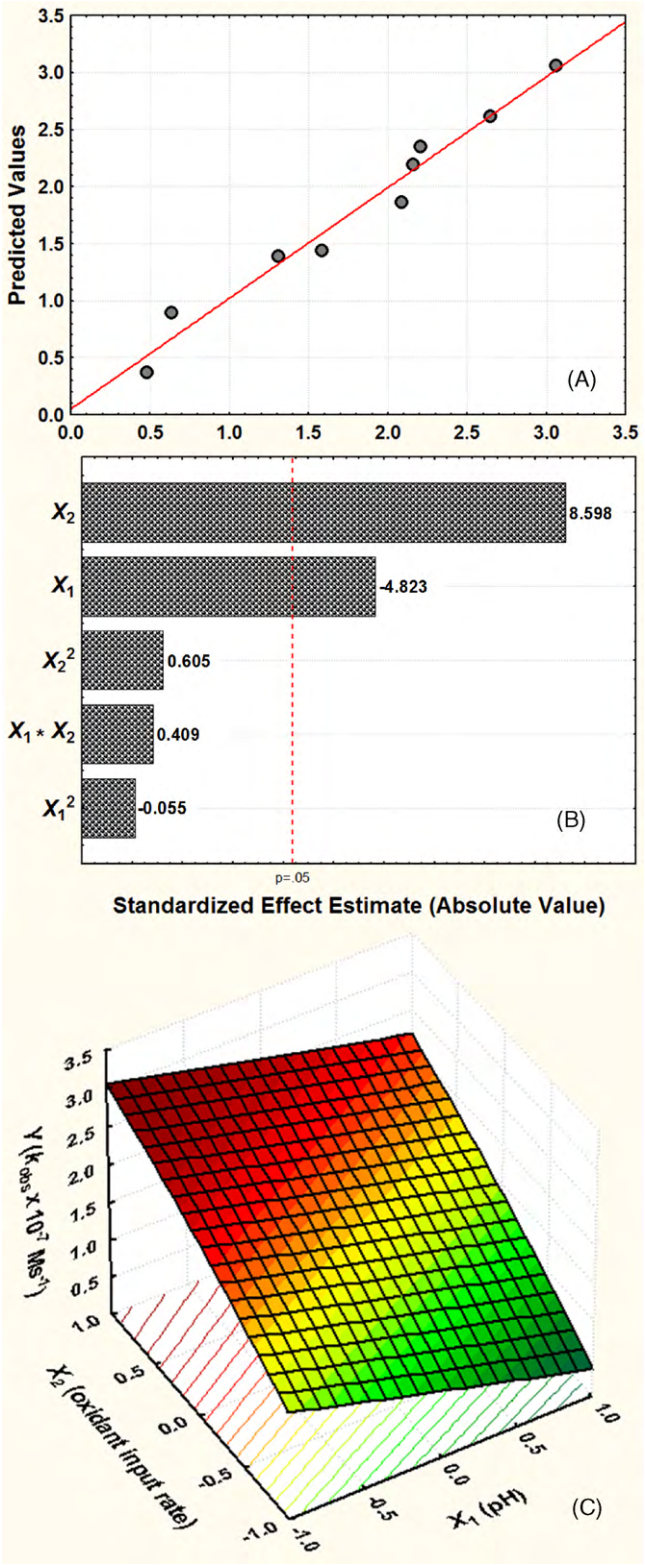

Fig. 7. Graphical evaluation of model M3 performance for the prediction of zero-order mineralization rate constant of AO7 model wastewater by UV/$S_2O_8^{2-}$ process: (A) observed *vs.* predicted plot, (B) Pareto chart, and (C) 3D response surface and contour plot.

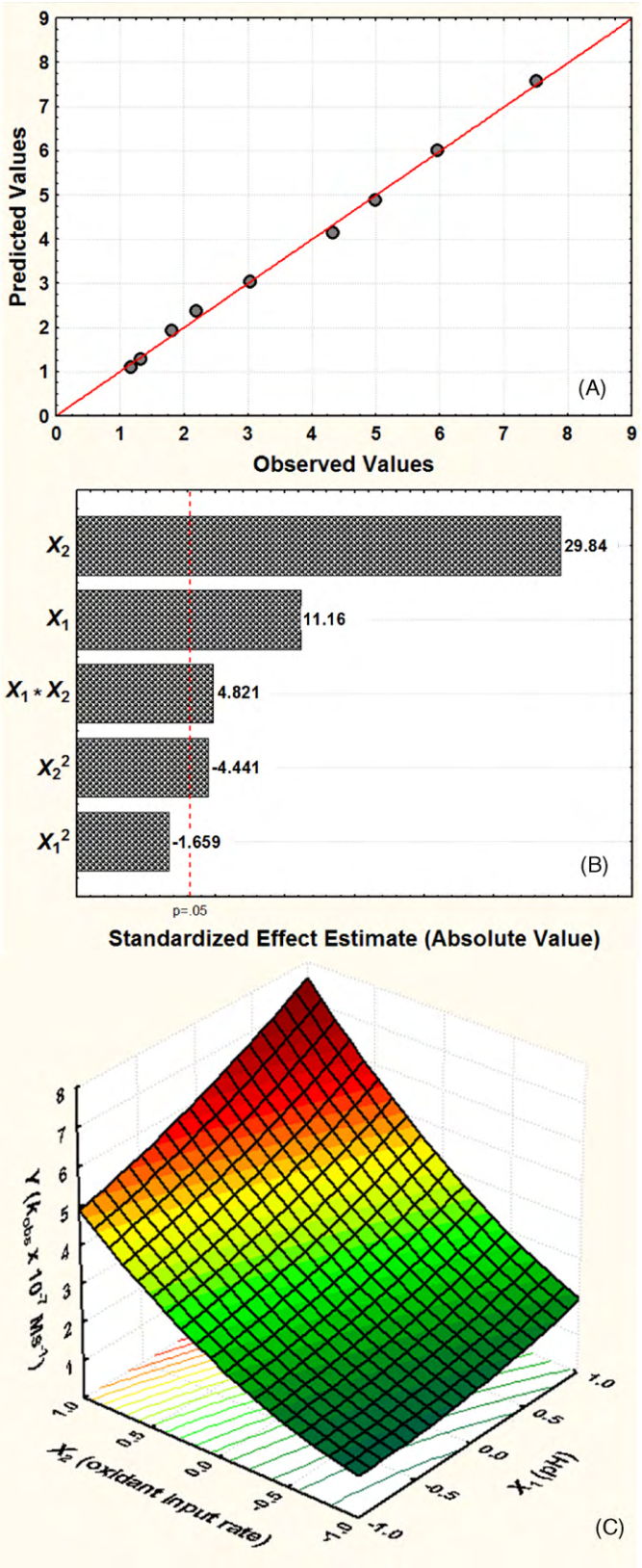

Fig. 8. Graphical evaluation of model M4 performance for the prediction of zero-order mineralization rate constant of AO7 model wastewater by UV/O_3 process: (A) observed *vs.* predicted plot, (B) Pareto chart, and (C) 3D response surface and contour plot.

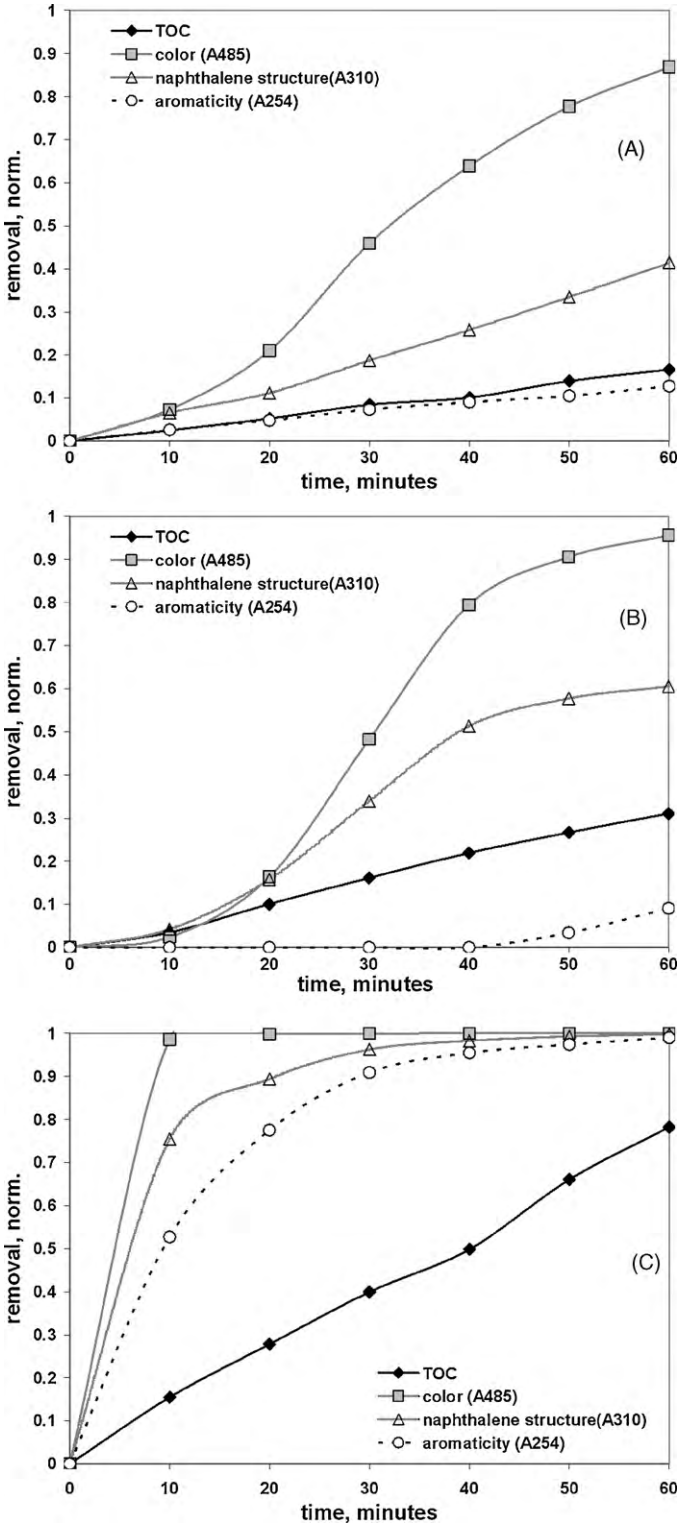

Fig. 9. Comparison of effectiveness studied processes performed at conditions determined as optimal within the investigate ranges: (A) UV/H_2O_2 process (pH_0 4.5 and oxidant input rate of 0.6 mM min^{-1}), (B) UV/$S_2O_8^{2-}$ process (pH_0 3 and oxidant input rate of 0.6 mM min^{-1}) and (C) UV/O_3 process (pH_0 10 and oxidant input rate of 0.6 mM min^{-1}) (the lines are only for connecting points and are not model results).

model components can be seen from the linear shape of 3D surface plot presented in Fig. 7(C). According to the elevation of predicted mineralization rates in dependence of initial pH at the set oxidant input rate (e.g. 0.6 mM min^{-1}, coded $X_2 = 1$) and *vice versa*, varying of input rate at the constant initial pH, one can conclude that oxidant input rate influences process behavior more significantly than the initial pH. A faster elevation of predicted AO7 mineralization rates was observed when changing the input rate at constant initial pH value in the comparison to opposite case (Fig. 7(C)). The same is indicated by Pareto chart (Fig. 7(B)), where bar for X_2 (input rate) is almost double longer than that for X_1 (initial pH). Furthermore, the negative coefficient of X_1 (Fig. 7(B)) indicates its unfavorable or antagonistic effect on the mineralization rate [21], i.e. higher pHs yielded with lower mineralization rates, as it can be observed from 3D surface plot (Fig. 7(C)). Other significant model component X_2 has a positive coefficient in Pareto chart (Fig. 7(B)), possessing the favorable or synergistic effect on mineralization rate. This means that AO7 mineralization rate would increase by increasing the reactor input oxidant concentration, as it can be clearly observed from Fig. 7(C). The optimal conditions within the investigated range of studied parameters of UV/$S_2O_8^{2-}$ process are located at the lowest level of factor X_1 (initial pH) and the highest level of factor X_2 (oxidant input rate). Therefore, the highest mineralization rate of AO7 model wastewater, $k_{obs} = 3.060 \times 10^{-7}$ M s^{-1}, by UV/$S_2O_8^{2-}$ process is achieved at initial pH 3 and oxidant input rate of 0.6 mM min^{-1}. It can be expected that an increase of oxidant input rate over that used in the study for the highest level would cause favorable effect on the mineralization rate, while the same cannot be expected for the decreasing of initial pH. Although M3 model predicts such a trend, this is not favorable from the environmental point of view due to the strong conditioning of wastewater to pHs below 3 prior the treatment. This could require the strong conditioning after the treatment as well, which could cause rather high concentration of unnecessary counter ions in the system presumably demanding further treatment. Consequently, the cost of the treatment would increase due to the high consumption of chemicals which is unfavorable on the industrial scale and additionally due to the possible demands for secondary treatment.

The third photooxidation process evaluated was UV/O_3. The RSM model M4 is developed in the same manner as in the cases of UV/H_2O_2 and UV/$S_2O_8^{2-}$ processes, and is presented by the following equation (11):

$$Y = 3.035 + 0.883 \times X_1 + 0.227 \times X_1^2 + 2.36 \times X_2 + 0.608 \times X_2^2 + 0.467 \times X_1 \times X_2 \quad (11)$$

The significance of model M4 and its components is characterized and the results are presented in Table 3 and Fig. 8. M4 possess the highest F (212.12) and lowest p (0.0005) values, as well as the highest regression coefficients ($R^2 = 0.997$ and $R^2_{adj} = 0.993$) among values obtained for models M2, M3 and M4. The excellent correlation of observed and predicted data by M4 is clearly visible from Fig. 8(A); all points are attached in some extent to the diagonal line. The results presented in Pareto chart (Fig. 8(B)) shows that all M4 components except X_1^2 are significant for the prediction of AO7 mineralization rates by UV/O_3 process. According to the lengths of the bars in plot, the most significant model M4 components are those linear ones (X_1 and X_2), and then their interaction term ($X_1 \times X_2$). However, from the 3D surface plot (Fig. 8(C)), it is evident that the quadratic model component contribute as well: the elevation of AO7 mineralization rate when changing one parameter and keeping other constant showed polynomial shape. Furthermore, the elevation of AO7 mineralization rate is more favorable when changing the oxidant input rate to higher values than the initial pH value to more basic conditions keeping the other parameter at the constant value. This is in accordance with the results

presented in Pareto chart where X_2 model component is associated with the longest bar in the chart (Fig. 8(B)). However, the difference between the influences of these two parameters on the mineralization rates is decreasing when values of these two parameters approached to their top levels used in the study. This observation favors the existence of an additional source of reactive species at higher pH values; HO• produced by catalyzed decomposition of ozone (Eq. (7)). Similarly like in the case of peroxidisulfate case (Fig. 7(C)), the optimal conditions within the investigated range of chosen process parameters are at the boundary levels. Both are located at the top levels of factors X_1 and X_2 (Fig. 8(C)), i.e. pH 10 and oxidant input concentration 0.6 mM min^{-1}. With these set conditions AO7 model wastewater was mineralized with the highest rate among all studied processes, possessing the zero-order rate constant $k_{obs} = 7.507 \times 10^{-7}$ M s^{-1}. According to the model M4 prediction, it can be assumed that mineralization would proceed at higher rate by increasing the oxidant input concentration over that chosen for top level in this study. The model predicts the same for an increase of initial pH values as well. However, like in the case of peroxidisulfate, it can be expected that increase of pH over studied 10, would have positive effect from environmental and economical point of view only up to certain point, i.e. initial pHs over 11 can be considered as unfavorable due to the very strong conditioning required before and presumably after the treatment.

3.4. Evaluation of the cost-efficiency of studied processes

In the final step of the study, processes at the optimal conditions determined above were compared on the basis of eco- and cost-effectiveness. It should however be pointed out that these conditions are optimal within the investigated ranges applied. Eco-criteria considered are: the decolorization of AO7 model wastewater (A_{485} for dye chromophore), degradation of dye monitored through decreases of absorbance of characteristic peaks for dye molecule (A_{310} for naphthalene structure and A_{254} for aromaticity) and the mineralization of organic content of AO7 model dye wastewater (Fig. 9), while under cost-criteria evaluation of operating cost is considered. As shown in Fig. 9, only UV/O_3 process yielded complete decolorization, which occurred within 10 min of treatment (Fig. 9(C)). Other two processes studied provided only partial decolorization of AO7 model wastewater; 87 and 96% in the cases of UV/H_2O_2 (Fig. 9(A)) and $UV/S_2O_8^{2-}$ (Fig. 9(B)) processes, respectively. Furthermore, for all studied eco-criteria, except for A_{254}, process effectiveness followed decreasing trend: $UV/O_3 > UV/S_2O_8^{2-} > UV/H_2O_2$, e.g. for mineralization rates 7.507×10^{-7} M $s^{-1} > 3.060 \times 10^{-7}$ M $s^{-1} > 1.555 \times 10^{-7}$ M s^{-1}. The discrepancy is observed with A_{254} (decreasing trend: $UV/O_3 > UV/H_2O_2 > UV/S_2O_8^{2-}$), which can potentially be explained by the interference of the dye peak at 254 nm through introduction of the peroxidisulfate oxidant [30]. Esplugas et al. [39] stated that pseudo first-order rate constants and half-life time, $t_{1/2}$, present global parameters including all phenomena involved in the studied process, and allow the overall comparison between the different AOPs. However, it was observed that processes studied when oxidant is continuously introduced in the system failed to follow the first-order kinetic for the chosen eco-criteria, mineralization, and that they follow zero-order kinetics (Fig. 3). Thereby, for the evaluation of the processes on the basis of cost-criteria, i.e. operating costs, the obtained zero-order reaction rates were considered. The costs of used reagents valid for Croatian market are given in Table 4. Values of $t_{1/2}$ and $t_{3/4}$, presenting times required to decrease overall organic content of AO7 model wastewater to half and quarter the amount present before reaction, respectively, are given in Table 5. When the values of $t_{3/4}$ are equal to $t_{1/2} \times 2$, it is possible to conclude that reactions obey first-order rate constants [39]. However, as it was stated above, that was not the case in our study (Table 5). Besides $t_{1/2}$ and $t_{3/4}$ and the corresponding costs to achieve the mineralization of AO7 model wastewater for these criteria, t^* and t^{**} and their corresponding costs were also calculated (Table 5). Newly included time criteria t^* represents the time required to achieve reference value of 15 mg C L^{-1} which is allowed to be discharged into the natural effluents of the second category (non-potable water) according to the Croatian legislation for water quality regulation [40]. Another time criteria t^{**} included represents the time required to achieve the complete mineralization. It is worth of noting that our previous study showed that when oxidant is introduced in the system at the constant rate, the complete mineralization could be achieved with the rate obeying the zero-order kinetic [12]. However, the slight discrepancy from zero-order kinetics can be expected when lower C-atoms by-products of dye degradation (e.g. oxalic and formic acid) would prevail in the remained organic content of treated wastewater due to the fact that their rate constants with HO• are two or three orders of magnitude lower than those of higher C-atoms by-products (aromatic compounds, e.g. phenolic compounds, or higher C-atoms aliphatic acids, e.g. maleic acid, fumaric acid, etc.) [20]. From the results presented in Fig. 9, it can be seen that UV/O_3 process seems to be the most efficient among studied processes, possessing the highest zero-order mineralization rate resulting with the achievement of chosen time criteria within the shortest treatment period (Table 5). However, when comparing the operating costs to achieve those time criteria, it can be observed that UV/H_2O_2 process was shown to be 1.6 times less expensive than UV/O_3 process (Table 5). Moreover, several additional reasons strongly favor the application of UV/H_2O_2 process for AO7 model wastewater treatment over UV/O_3, but could be valid in general as well. (i) The initial pH of application; weak acidic in the case of UV/H_2O_2 instead of strong basic conditions in the case when ozone is used as an oxidant seems to be a better option. (ii) No requirements for the removal of oxidant in excess during the treatment; in the case of ozone a catalytic decomposition of ozone reactor outlet stream is highly required [14,39]. (iii) Presumably lower costs of treat-

Table 4
Cost of reagents used in applied processes (costs are given in euros and the values are valid for Croatian market).

Reagents	Basis	Cost (EUR)
H_2O_2, 30%	1 L	9.724
NaS_2O_8, p.a.	500 g	52.518
O_2, >99.9%	100 L	0.206
Electricity	1 kWh	0.081

Table 5
Cost evaluation for all applied processes (processes conducted in laboratory scale batch reactor).

Process	$k_{obs} \times 10^{-7}$ (M s^{-1})	$t_{1/2}$ (min)	Cost (EUR)	$t_{3/4}$ (min)	Cost (EUR)	t^* (min)	Cost (EUR)	t^{**} (min)	Cost (EUR)	Overall cost (EUR g^{-1})
UV/H_2O_2	1.555	187.0	0.058	280.5	0.087	240.0	0.075	374.0	0.116	2.772
$UV/Na_2S_2O_2$	3.060	95.0	0.714	142.5	1.070	122.0	0.916	190.0	1.427	33.98
UV/O_3	7.507	38.7	0.093	58.1	0.139	49.7	0.119	77.5	0.186	4.424

t^* time required to achieve reference value of 15 mg C L^{-1} allowed to be discharge to the natural resource of first category according to the Croatian legislation [40].
t^{**} time required to achieve complete mineralization.

ment process equipment installation and maintaining; in UV/O_3 process the installation costs for ozone generator could rapidly increase the initial investment costs. However, it should be emphasized that the evaluation of operating costs has been made on the basis of laboratory scale investigations. The overall costs are represented by the sum of capital, operating and maintenance costs. For a full-scale system these costs would, aside from the nature and the concentration of pollutants, strongly depend on the flow rate of the effluent and the configuration of the reactor [14].

4. Conclusions

The study compared the effectiveness of several photooxidation processes for the treatment of wastewater containing azo dye C.I. Acid Orange 7 as a model pollutant. The process efficiency is estimated on the basis of the following criteria: decolorization efficiency, dye degradation efficiency (monitored over the decrease of several characteristic peaks in AO7 UV/vis spectra) and mineralization of organic content of AO7 model wastewater. The influence of cross-factor effects of studied process parameters (initial pH, the concentrations of oxidant in the reactor inlet stream, and the type of oxidant) was investigated using full factorial design with three factors (two numeric and one categorical) at three levels combined with response surface modeling (RSM). The ANOVA results (R^2, F, p) showed high accuracy of developed quadratic model M1 in predicting the zero-order mineralization rate constants of AO7 model wastewater. Among studied process parameters, the type of oxidant and the concentration of oxidant in the reactor inlet stream were shown to be most influencing parameters on the performance of studied photooxidation processes. The highest rate of mineralization of AO7 model wastewater, $k_{obs} = 7.507 \times 10^{-7}$ M s^{-1}, was obtained for the photooxidation process using ozone as an oxidant at the initial pH 10 and oxidant reactor input rate of 0.6 mM min^{-1}. Aside from the 78.3% mineralization achieved after 60 min of treatment, the complete decolorization within 10 min of treatment and the complete degradation of naphthalene structures within 60 min of treatment were obtained. The results of the study indicate that the type of oxidant is the most important factor due to the synergy of several effects: (i) its capability to form radical species responsible for the degradation of organic pollutants (either by direct photolysis or catalyzed by process conditions), and (ii) its capability to degrade present organic pollutants directly by itself.

The same RSM methodology was used in order to establish the optimal conditions within the investigated range for each of the photooxidation processes studied in order to evaluate the cost-effectiveness (operating costs). The effectiveness of applied processes (UV/H_2O_2, $UV/S_2O_8^{2-}$ and UV/O_3) performed at the conditions determined as optimal within the investigated range of studied process parameters was compared. The process effectiveness on the basis of studied eco-criteria (highest yield of AO7 degradation according to all monitored criteria) followed decreasing trend: $UV/O_3 > UV/S_2O_8^{2-} > UV/H_2O_2$, However, comparison of the operating costs for each process showed that UV/H_2O_2 process (2.772 EUR g^{-1}) is 1.6 times less expensive than UV/O_3 process (4.424 EUR g^{-1}) for the mineralization of organic content of AO7 model wastewater. However, it should be emphasized that this evaluation of operating costs has been made on the basis of laboratory scale investigations and could be taken just as an indicator, not the general rule. The findings of the current study are intended to be used in the future study aimed on developing of the mathematical models for describing the behavior of these treatment processes, both in batch and semi-batch systems.

Acknowledgement

We would like to acknowledge on the financial support both from the Ministry of Science, Education and Sport, Republic of Croatia (Project #125-1253092-1981).

References

[1] K. Hunger, Industrial Dyes: Chemistry, Properties and Applications, John Wiley and Sons–VCH, New York, USA, 2003.
[2] H. Zollinger, Color Chemistry: Syntheses, Properties and Applications of Organic Dyes and Pigments, Wiley–VCH, Weinheim, Germany, 2003.
[3] E. Forgacs, T. Cserhati, G. Oros, Removal of synthetic dyes from wastewaters: a review, Environ. Int. 30 (2004) 953–971.
[4] S. Karcher, A. Kornmuller, M. Jekel, Anion exchange resins for removal of reactive dyes from textile wastewaters, Water Res. 36 (2002) 4717–4724.
[5] D.T. Sponza, M. Işik, Decolorization and azo dye degradation by anaerobic/aerobic sequential process, Enzyme Microb. Technol. 31 (2002) 102–110.
[6] K. Shakir, A.F. Elkafrawy, H.F. Ghoneimy, S.G.E. Beheir, M. Refaat, Removal of rhodamine B (a basic dye) and thoron (an acidic dye) from dilute aqueous solutions and wastewater simulants by ion flotation, Water Res. 44 (5) (2010) 1449–1461.
[7] S. Papić, N. Koprivanac, A. Lončarić Božić, A. Meteš, Removal of some reactive dyes from synthetic wastewater by combined Al(III) coagulation/carbon adsorption process, Dyes Pigm. 62 (2004) 293–300.
[8] F.A.P. Costa, E.M. dos Reis, J.C.R. Azevedo, J. Nozaki, Bleaching and photodegradation of textile dyes by H_2O_2 and solar or ultraviolet radiation, Solar Energy 77 (2004) 29–35.
[9] G.L. Baughman, E.J. Weber, Transformation of dyes and related compounds in anoxic sediment: kinetics and products, Environ. Sci. Technol. 28 (2) (1994) 267–276.
[10] I. Arslan, I.A. Balcioglu, Degradation of commercial reactive dyestuffs by heterogenous and homogenous advanced oxidation processes: a comparative study, Dyes Pigm. 43 (1999) 95–108.
[11] M. Neamtu, A. Yediler, I. Siminiceanu, M. Macoveanu, A. Kettrup, Decolorization of disperse red 354 azo dye in water by several oxidation processes—a comparative study, Dyes Pigm. 60 (1) (2004) 61–68.
[12] I. Peternel, N. Koprivanac, H. Kusic, UV-based processes for reactive azo dye mineralization, Water Res. 40 (2006) 525–532.
[13] R. Gogate, B. Pandit, A review of imperative technologies for wastewater treatment I: oxidation technologies at ambient conditions, Adv. Environ. Res. 8 (2004) 501–551.
[14] S. Parsons, Advanced Oxidation Processes for Water and Wastewater Treatment, IWA Publishing, London, England, 2004.
[15] H. Kusic, N. Koprivanac, L. Srsan, Azo dye degradation using Fenton type processes assisted by UV irradiation: a kinetic study, J. Photochem. Photobiol. A 181 (2–3) (2006) 195–202.
[16] F.J. Beltran, Ozone-UV radiation-hydrogen peroxide oxidation technologies, in: M.A. Tarr (Ed.), Chemical Degradation Methods for Wastes and Pollutants, Environmental and Industrial Applications, Marcel Dekker, Inc., New York, USA, 2003, pp. 1–77.
[17] N.L. Frigon, D. Mathews, Practical Guide to Experimental Design, John Wiley and Sons, New York, USA, 1997.
[18] D.C. Montogomery, Design and Analysis of Experiments, John Wiley and Sons, New York, USA, 2005.
[19] R.H. Myer, D.C. Montogomery, Response Surface Methodology: Process and Product Optimization using Designed Experiment, 2nd ed., John Wiley and Sons, New York, USA, 2002.
[20] P. Kralik, H. Kusic, N. Koprivanac, A. Loncaric Bozic, Degradation of chlorinated hydrocarbons by UV/H_2O_2: the application of experimental design and kinetic modeling approach, Chem. Eng. J. 158 (2010) 154–166.
[21] K. Yetilmezsoy, S. Demirel, R.J. Vanderbei, Response surface modeling of Pb(II) removal from aqueous solution by Pistacia vera L.: Box–Behnken experimental design, J. Hazard. Mater. 171 (2009) 551–562.
[22] S. Ray, J.A. Lalman, N. Biswas, Using the Box–Behnken technique to statistically model phenol photocatalytic degradation by titanium dioxide nanoparticles, Chem. Eng. J. 150 (2009) 15–24.
[23] P.A. Soloman, C. Ahmed Basha, M. Velan, N. Balasubramanian, P. Marimuthu, Augmentation of biodegradability of pulp and paper industry wastewater by electrochemical pre-treatment and optimization by RSM, Sep. Purif. Technol. 69 (1) (2009) 109–117.
[24] I. Arslan-Alaton, G. Tureli, T. Olmez-Hanci, Treatment of azo dye production wastewaters using Photo-Fenton-like advanced oxidation processes: Optimization by response surface methodology, J. Photochem. Photobiol. A 202 (2–3) (2009) 142–153.
[25] K. Venkataraman, The Chemistry of Synthetic Dyes, Academic Press, New York, USA, 1970.
[26] I. Nicole, J. De Laat, M. Dore, J.P. Duguet, C. Bonnel, Utilisation du rayonnement ultraviolet dans le traitement des eaux: mesure du flux photonique par actinometrie chimique au peroxyde d'hydrogene: use of U.V. radiation in water treatment: measurement of photonic flux by hydrogen peroxide actinometry, Water Res. 24 (2) (1990) 157–168.
[27] K.A. Connors, Chemical Kinetics: The Study of Reaction Rates in Solution, Wiley–VCH, New York, USA, 1990.

[28] Stat-Ease, Multifactor RSM Tutorial (Part 2—Optimization), Design-Expert software Version 7.1.5 User's Guide, 2008.
[29] G.E.P. Box, D.R. Cox, An analysis of transformations, J. R. Stat. Soc. B Stat. Methods 26 (1964) 211–246.
[30] D. Kamel, A. Sihem, C. Halima, S. Tahar, Decolourization process of an azoique dye (Congo red) by photochemical methods in homogeneous medium, Desalination 247 (2009) 412–422.
[31] S. Papić, N. Koprivanac, A. Lončarić Božić, D. Vujević, S. Kučar Dragičević, H. Kušić, I. Peternel, AOPs in azo dye wastewater treatment, Water Environ. Res. 78 (6) (2006) 572–579.
[32] H. Tomiyasu, H. Fukutomi, G. Gordon, Kinetics and mechanism of ozone decomposition in basic aqueous solution, Inorg. Chem. 24 (19) (1985) 2962–2966.
[33] K.-C. Huang, R.A. Couttenye, G.E. Hoag, Kinetics of heat-assisted persulfate oxidation of methyl tert-butyl ether (MTBE), Chemosphere 49 (2002) 413–420.
[34] R.E. Huie, C.L. Clifton, P. Neta, Electron transfer reaction rates and equilibria of the carbonate and sulfate radical anions, Int. J. Rad. Appl. Instrum. C Rad. Phys. Chem. 38 (1991) 477–481.
[35] K.L. Ivanov, E.M. Glebov, V.F. Plyusnin, Yu.V. Ivanov, V.P. Grivin, N.M. Bazhin, Laser flash photolysis of sodium persulfate in aqueous solution with additions of dimethylformamide, J. Photochem. Photobiol. A 133 (2000) 99–104.
[36] S. Guittonneau, J. DeLaat, M. Dore, Kinetic-study of the photodecomposition rate of aqueous ozone by UV irradiation at 253.7 nm, Environ. Technol. 11 (5) (1990) 477–490.
[37] S. Guittonneau, J. DeLaat, J.P. Duguet, C. Bonnel, M. Dore, Oxidation of parachloronitrobenzene in dilute aqueous-solution by O_3 + UV and H_2O_2 + UV—a comparative-study, Ozone Sci. Eng. 12 (1) (1990) 73–94.
[38] R. Alnaizy, A. Akgerman, Advanced oxidation of phenolic compounds, Adv. Environ. Res. 4 (3) (2000) 233–244.
[39] S. Esplugas, J. Gimenez, S. Contreras, E. Pascual, M. Rodriguez, Comparison of different advanced oxidation processes for phenol degradation, Water Res. 36 (2002) 1034–1042.
[40] State Office for Waters, Directive on amendments of regulations for limit values of hazardous substances and other indicators in wastewater, The Official Gazette 6 (2001) (January 24, 2001), Croatia.